Noninvasive Therapeutic Evaluation on Rodent Liver Tumor Treated with Vascular Disrupting Agent: Multiparametric Magnetic Resonance Imaging in Correlation with Microangiography and Histology

H. Wang[1], J. Li[1], F. Chen[1], and Y. Ni[1]

[1]Catholic University of Leuven, Leuven, East Flanders, Belgium

Objectives: To document tumoricidal events after intravenous administration of a vascular targeting agent ZD6126 in rodent liver tumors by using multiparametric magnetic resonance imaging (MRI) and F-18 fluorodeoxyglucose-micro-positron emission tomography (^{18}F-FDG micro-PET) in correlation with postmortem microangiography and histopathology.

Materials and Methods: Forty rhabdomyosarcomas of 8-14 mm in diameter were obtained 16 days after implantation into liver lobes of 20 rats and randomly assigned into control and treated groups. Using a 1.5T Siemens Symphony magnet and a 4-channel wrist coil, T2-weighted imaging (T2WI), pre-contrast T1-weighted imaging (T1WI) and contrast-enhanced T1WI (CE-T1WI), diffusion-weighted imaging (DWI), and dynamic contrast-enhanced MRI (DCE-MRI) were acquired at pre-treatment baseline, 1h, 24h and 48h after *iv* injection of ZD6126 at 50 mg/kg and vehicle in 15 treated (n = 30) and 5 control rats (n = 10), respectively. Micro-PET was performed at the pretreatment baseline and 24h after the treatment, respectively. *In vivo* MRI data including signal intensity (SI), tumor volume, DWI-derived apparent diffusion coefficient (ADC), DCE-MRI-derived volume transfer constant per unit volume of tissue, K, and maximal initial slope (MIS) of contrast-time curve (CTC), and PET data including mean standardized uptake value of FDG (SUV_{mean}) and total lesion glycolysis (TLG), were correlated with *ex vivo* microangiography with digital mammographic unit and micro-computed tomography (micro-CT) and histopathological findings.

Results: ZD6126-treated tumors grew slower than those of controls ($P < 0.05$), with vascular shutdown evident on CE-T1WI at 1h but more prominent at 24h (Fig. 1, 2). However, enhanced rim occurred in the periphery 48h after treatment, indicating neovascularization (Fig. 2). ADC map enabled distinction between necrotic and viable tumors (Fig. 2, 3). K and MIS significantly decreased at 1h though 24h, and partly recovered at 48h (Fig. 4). SUV_{mean} and TLG significantly reduced at 24h after ZD6126 treatment ($P < 0.05$) (Fig.1, 2). ZD6126 selectively targeted at tumoral vessels while normal liver was not affected. MRI and PET findings were verified by postmortem microangiographic and histopathological techniques (Fig. 2).

Conclusions: Clinical MRI allowed monitoring of ZD6126-related vascular shutdown, necrosis, and neovascularization of liver tumors in rats. Single dose of ZD6126 appeared insufficient for tumor eradication due to evident peripheral residue and recurrence.

References

1. Evelhoch JL, et al. ***Clin Cancer Res***. 2004; 10(11):3650-3657.
2. Beerepoot LV, et al. ***J Clin Oncol.*** 2006; 24(10):1491-1498.
3. Chen F, et al. ***Radiology*** 2006; 239(2): 554-562.

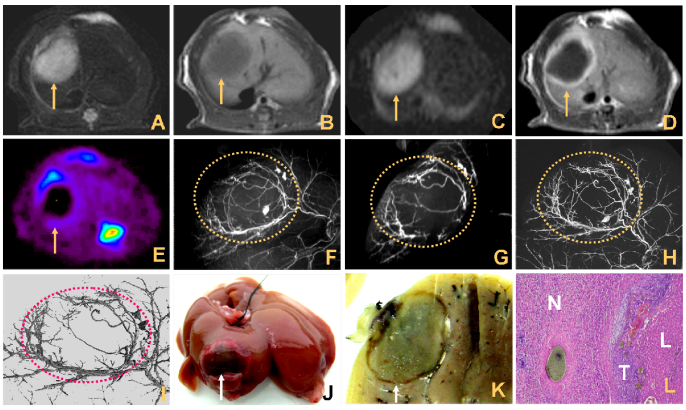

Fig. 2 Images after ZD6126 treatment and postmortem verifications were correlated. At 48h, there was no obvious change of SI on T2WI (A) and T1WI (B). However, SI in central part of tumor was higher due to central necrosis, while lower SI of peripheral part indicated the recurrence of tumor on ADC (C), which corresponded with the central un-enhanced area and ring enhancement on CE-T1WI, respectively (D). At 24h, FDG uptake was significantly decreased on micro-PET (E). Postmortem microangiography revealed that almost all of the vessels in the center disappeared with the plentiful neoangiogenesis emerging in the periphery of tumor (F), which was more prominent on 3-mm-thick sliced section (G). Micro-CT depicted the similar vascular shutdown effect of ZD6126 and tumoral recurrence on 3-dimenasional reconstruction with maximal intensity projection (H) and volumetric rendering (I), respectively. Macroscopically, liver specimen (J) and its 3-mm-thick sliced section (K) demonstrated the expansion pattern of tumor growth. Photomicrograph (L) confirmed the viable tumor (T), ZD6126-induced tumoral necrosis (N) and normal liver (L).

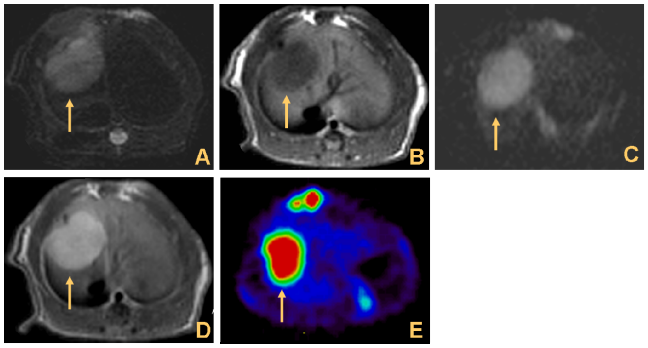

Fig. 1 Baseline images before ZD6126 treatment. The tumor showed homogenous hyperintensity on T2WI (A) and ADC (C), hypointensity on T1WI (B), and homogeneous enhancement on CE-T1WI (D). High uptake of FDG in tumor was observed on micro-PET (E).

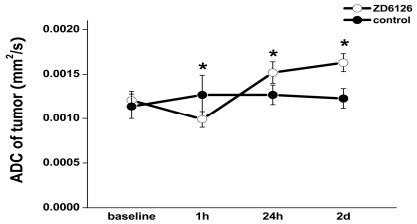

Fig. 3 Compared to the baseline, a significant drop of ADC at 1h after ZD6126 treatment indicated the swelling tumoral cells and subsequent constrained water mobility in the extracellular space after vascular shutdown. At 24h, a marked ADC increase suggested progressing necrosis in the center of tumor and the subsequent increased water mobility in the extracellular space. At 2 days, ADC kept increasing. * $P < 0.05$ ZD6126 vs. control.

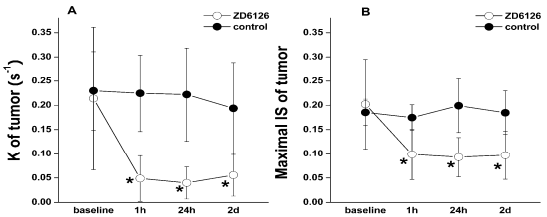

Fig. 4 Quantitative and semi-quantitative analyses of DCE-MRI showed that K (A), approximating the permeability of tumor, and MIS (B) significantly decreased from 1h through 24h after ZD6126 treatment, and partially recovered at 2 days, respectively. * $P < 0.05$ ZD6126 vs. control.